

Fault Tolerant Wind Farm Control - a Benchmark Model

Peter Fogh Odgaard and Jakob Stoustrup

Abstract—In the recent years the wind turbine industry has focused on optimizing the cost of energy. One of the important factors in this is to increase reliability of the wind turbines. Advanced fault detection, isolation and accommodation are important tools in this process. Clearly most faults are dealt with best at a wind turbine control level. However, some faults are better dealt with at the wind farm control level. In this paper a benchmark model for fault detection and isolation, and fault tolerant control of wind turbines implemented at the wind farm control level is presented. The benchmark model includes a small wind farm of nine wind turbines, based on a simple model of a wind turbine as well as the wind and interactions between wind turbines in the wind farm. The model includes wind and power references scenarios as well as three relevant fault scenarios. This benchmark model is used in an international competition dealing with Wind Farm fault detection and isolation and fault tolerant control.

I. INTRODUCTION

A consequence of the increased level of wind generated power in many power grids is that it becomes more and more important that the wind turbines/wind farms generating the energy are reliable. It must be ensured that the wind farms should be able to generate the maximum power allowed by the given wind speed for the wind farm all times. This means that occurring faults in the wind turbines in the wind farm should be detected, isolated and accommodated with the lowest influence on the generated power.

In the recent years' research, focus has turned to Fault Detection and Isolation (FDI) and Fault Tolerant Control (FTC) of wind turbines, some examples can be seen in [1] and [2]. In [3] a benchmark model was proposed for FDI and FTC on wind turbines. Based on this model an international competition on FDI and FTC have been proposed some of the contributions to the competition can be seen in [4] and [5].

On wind farm level, only a few works on condition monitoring and fault detection of wind turbines have been reported one example can be found in [6]. The idea in detection, isolation and accommodation of faults on a wind farm level, is that performance and operation of the different wind turbines in a given wind farm can be compared. This can for example be used to detect slowly developing faults, since they would show an increasing difference compared with other turbines operating under almost the same wind conditions. A benchmark model for FDI and FTC on Wind Farm level is consequently proposed as a supplement to the wind turbine benchmark model.

The typical control structure in a wind farm would be that each wind turbine is controlled with their own control system which also contains or could contain a FDI/FTC system. A controller is as well running at the wind farm

level typically with a lower sampling rate and usually with some communication delays. Faults which can be detected, isolated and accommodated at the wind turbine level would be faster accommodated on this level, but some faults are not so easily handled at the wind turbine level. These faults typically result in a slow decrease in the generated power, and it is difficult to determine if a power drop is due to a fault or a lower wind speed than expected only using data from one wind turbine. The benchmark model proposed in this paper represents a small wind farm with nine 4.8MW wind turbines, which are all described by second order models, and the interactions between the wind turbines are modeled by a simple wake model, which is based on previously published wind farm models. Three different faults are introduced on different wind turbines in the wind farm. The benchmark model proposed in this paper is used in an international competition on wind farm FDI and FTC, see [7].

In Section II the wind farm considered is described. The considered fault scenarios are introduced in Section III. The model of the wind farm including a simple wind turbine model is described in Section IV. In Section V the used test scenarios in this benchmark are defined. The paper is finalized by a summary in Section VI.

II. WIND FARM DESCRIPTION

In this benchmark model a simple wind farm with 9 wind turbines is considered. The layout of the farm is a square grid, as illustrated in Fig. 1. The distance between the wind turbines in both directions are 7 times the rotor diameter, L . Two measuring masts are located in front of the wind turbine, one in each of the wind directions considered in this benchmark model. At these measuring masts the wind speed is measured relatively undisturbed by the aerodynamics of the wind turbines. These measuring masts are located with a distance of 10 times L in front of the wind farm. The wind turbines in the farm are numbered by their row and column number as illustrated in Fig. 1. In this model a generic 4.8MW wind turbine is used: details on this model can be found in [3]. The turbine is a three bladed horizontal axis, pitch controlled variable speed wind turbine. Each of the wind turbines are described by simplified models including logic, variable parameters and 3 states. The states in the wind turbine models are: generated electrical power, P , collective pitch angle, β , and generator speed, ω_g , which are measured and provided to the wind farm controller. Notice that only one measured pitch angle is assumed to provide since the wind turbine controller provides the same pitch reference to all three pitch actuators.

The two scenarios with different wind directions are both driven by the same wind speed sequence (possibly with a

Peter Fogh Odgaard is with Automation & Control, Department of Electronic Systems, Aalborg University, Aalborg, Denmark pfo@es.aau.dk
Jakob Stoustrup is with Automation & Control, Department of Electronic Systems, Aalborg University, Aalborg, Denmark

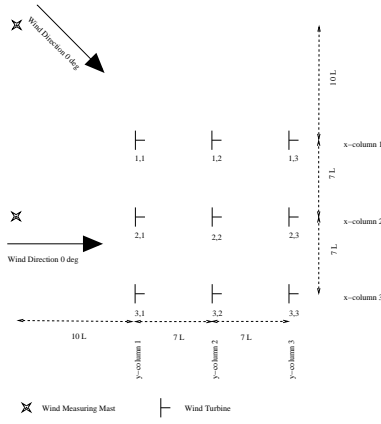


Fig. 1. Illustration of the layout of the example wind farm. It is a farm of 9 turbines in square grid. The measuring masts are placed in front of the wind farm in the two wind directions considered, e.g. 0 deg and 45 deg.

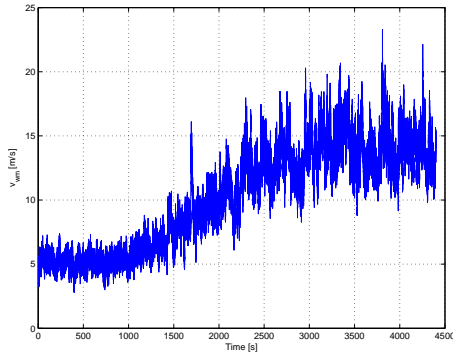


Fig. 2. The wind speed sequence seen at the measuring mast.

time shift) at the measuring masts. The wind sequence can be seen from Fig. 2. The sequence is 4400 s long and contains a wind speed increase from 5 m/s to 15 m/s in mean value and peak value at 23 m/s. In this benchmark model a very simple wind farm controller is used. It provides the wind turbine controllers with a power reference. It works by distributing power references to the wind turbines. The reference to each wind turbine is the power reference to the wind farm divided by the number of wind turbines in the wind farm fed through a low pass filter.

III. FAULT SCENARIOS

In this benchmark, three faults are considered which influence the three measured variables from the wind turbine: P , β , ω_g . It is also assumed that these faults can be detected at the wind farm level, and they are also difficult to detect at within the wind turbines. These faults are also known to be problematic based on proprietary sources in the wind turbine industry.

Fault 1: Fault 1 is debris build-up, due to dirt, etc., on the blades which changes the aerodynamics of the wind turbine, typically by lowering the maximally obtained power. It is difficult to detect this fault in the wind turbine, since it is difficult to determine if a lower generated power is due to debris on the blades or simply that the wind speed is lower than measured/estimated. More details on this fault can be

seen in [8].

Fault 2: Fault 2 is due to a misalignment of one or more blades originated at the time of installation of the wind turbine. This leads to an offset between the measured and actual pitch angle for one or more blades, and introduces as well a difference between the blade loads for the different blades at the same rotational position, which can excite structural modes. It will also result in a slightly different rotational speed of the turbine compared with a non-faulty case. The wind turbine controller will compensate for the last effect by adjusting all the pitch angles with the same value such that the generator speed is at the requested value, but compared with other wind turbines it will operate with a slightly different pitch angle for the same wind conditions.

Fault 3: Fault 3 is a change in the drive train damping due to wear and tear. The state-of-the-art as today is to use condition monitoring on the drive train to detect changes in frequency spectra of different vibration measurements etc. It is clearly relevant to investigate if the same can be obtained using the measurements available in the control systems either on wind turbine or wind farm level. In [9] a number of contributions to the wind turbine FDI benchmark problem in [3] were reviewed and analyzed, and it is concluded that the FDI solution proposed is not suitable for FDI of the drive train damping on a wind turbine level. It is therefore very relevant to investigate this fault on a wind farm level.

Fault Detection and Isolation Requirements: It is critical to detect and isolate all these faults, i.e. no missed detections are allowed. All faults should be detected within 3 s. It is important that the number of false positive detections and isolation are low, and there should at least in average be 1000 s between false positive detections and isolations, and the false positive detection must maximally be detected and isolated within three successive samples.

Monte Carlo studies are expected to be applied to verify that the proposed schemes can detect and isolate the faults and that they are robust towards measurement noises, etc. The simulation should be repeated 100 times, using different seeds in the stochastic parts.

The FDI scheme should be implemented in the FDI block in the Simulink implementation of the benchmark model, which can be obtained from [10]. A detected and isolated fault should activate the respective binary detection and isolation signals. All available signals are fed into this block.

Fault Tolerant Control Requirements: All faults should be accommodated as soon as they are detected and isolated. In case of all three faults the power references to the wind turbines should be reset such that the power reference to the wind farm is followed. In case of Fault 2 and Fault 3, relevant load damage should be minimized. These damage signals are provided by the Damage Equivalent Computer block in the Simulink model. Please notice that the outputs of this block is not available for FDI or FTC algorithms, they are only available for evaluation of the schemes. The total wind farm damage due to Fault 2 and Fault 3 are respectively denoted as γ_2 and γ_3 .

Damage of Fault 2 at each wind turbine at a given time is

modeled as following. A ratio between the pitch offset due to the fault and the fault free pitch angle is computed. This ratio is limited to the interval between 0 and 1, where 1 is obtained for small fault free pitch angles, and where pitch offset is present as well. This is given as an equation in (1).

$$\hat{\gamma}_{2,N}[n] = \begin{cases} 0 & \text{if } \frac{\beta_{fo,N}[n]}{\beta_{ff,N}[n]} \leq 0 \\ \frac{\beta_{fo,N}[n]}{\beta_{ff,N}[n]} & \text{if } 0 < \frac{\beta_{fo,N}[n]}{\beta_{ff,N}[n]} < 1, \\ 1 & \text{if } \frac{\beta_{fo,N}[n]}{\beta_{ff,N}[n]} \geq 1 \end{cases}, \quad (1)$$

where $\beta_{fo,N}[n]$ is the fault offset on the blade pitch angle with the wind turbine N , and $\beta_{ff,N}[n]$ is the fault free pitch angle in the wind turbine N .

This ratio is subsequently multiplied with the cube of the ratio between the actual and nominal wind speed, (v_w and v_{num}). For numerical reasons this value is after wards scaled with a factor of K_{γ_2} , see (2).

$$\gamma_{2,N} = (K_{\gamma_2} \cdot \hat{\gamma}_{2,N}[n] \cdot (v_w[n] - v_{nom})^2)^2, \quad (2)$$

where N is the wind turbine number.

The damage of Fault 2 for the entire wind farm is given by (3). γ_2 is obtained as the max of the square of the damage for Fault 2 for all wind turbines. The damage of this fault is modeled like this in order to model the damage due to unbalanced structural loads as a result of this pitch offset, including the cubic nature of the wind speed dependency.

$$\gamma_2[n] = \max_{i \in \{1,2,3\}, j \in \{1,2,3\}} (\gamma_{2,i,j}[n]). \quad (3)$$

Damage of Fault 3 at each wind turbine is modeled as the effective amplitude of the drive train oscillation, ξ_{dt} , multiplied with a factor, K_{γ_3} for numerical reasons and squared in order to obtain the damage of Fault 3 for the individual wind turbine, $\hat{\gamma}_{3,N}[n]$. The damage value is described by (4).

$$\hat{\gamma}_{3,N}[n] = (K_{\gamma_3} \cdot \xi_{dt})^2. \quad (4)$$

The total damage of the wind farm for Fault 3, $\gamma_3[n]$, is obtained as a sum of all $\hat{\gamma}_{3,N}[n]$, see (5).

$$\gamma_3[n] = \sum_{i \in \{1,2,3\}, j \in \{1,2,3\}} (\gamma_{3,i,j}[n]). \quad (5)$$

This models the damaging effects by the drive train oscillations to the wind turbine. The larger the oscillation the larger is the damage, since oscillation frequency is assumed to be constant. The parameters used in damage models can be found in Section IV-D.

The FTC scheme should be implemented in the Wind Farm controller block in the Simulink implementation. All available signals are fed into this block.

IV. WIND FARM MODEL

This model consists of 3 parts. A simple wind and wake model, which will be described in details in Sec. IV-A. This model represents a model of the wind in the wind farm, and thereby also models the interconnections between the wind turbines through the wakes. These wakes depends on how the wind turbines are controlled, so an upwind turbine can either

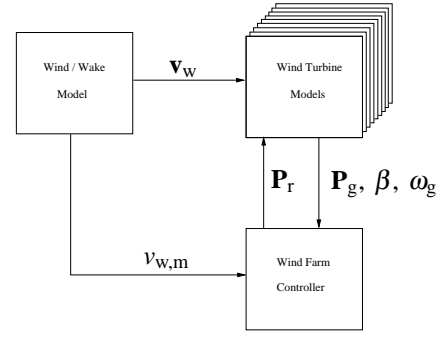


Fig. 3. Illustration of general model structure. Wind/Wake Model models the wind speed at the different wind turbines in the wind farm, and by the wake model represents the interactions between the wind turbines in the wind farm. Wind Turbine Models consists of nine separate models of the wind turbines in the wind farm. Wind Farm Controller distributes power references to the wind turbines in the wind farm in order to control the overall generated power.

increase or decrease the wake at the downwind turbine by the control actions. However in order to keep this benchmark model simple and low in computational requirements, it is assumed that the wakes are independent of the control of the individual wind turbines. A more detailed wind farm model obtained in the EU project - Aeolus for control design can e.g. be found in [11]. The simple wind turbine model which only contains a few states, can be seen in Sec. IV-B. The used wind farm controller is described in Sec. IV-C.

The general outline of the model can be seen from Fig. 3. In this figure the following variables are used. \mathbf{v}_w is a vector of wind speeds $v_{w,n}$ to each of the wind turbines, n indicates the wind turbine number, $v_{w,m}$ is the measured wind speed at the measuring mast, \mathbf{P}_r is a vector of power references to the wind turbines, $P_{r,n}$, \mathbf{P}_g is a vector of $P_{g,n}$ for each of the wind turbines, which is the generated electrical power, β is a vector of the pitch angle for each of the wind turbines, β_n , ω_g is a vector of the generator speed of the wind turbines, $\omega_{g,n}$. The model can be downloaded from [10].

A. Wind and Wake model

The wind in the model is driven by the wind sequence seen in Fig. 2. This wind sequence is used instead of a stochastic generated sequence since it contains the entire operation range of the wind turbines, and is as well known to be challenging. This wind sequence is used as the dominant wind speed, to which random noise is added to represent the wind turbulence. The wind sequence is delayed by the distance between the different points in the wind farm (measuring masts and wind turbines) and the mean wind speed. The distances depend on the wind direction. In the case of 0 degree wind direction the distance between the measuring mast and the first wind turbines are 1150m and between the wind turbine columns 805m. In the case of 45 degree wind direction the distance between the measuring mast and the first wind turbine 1626.35m and the distance between the wind turbines in the wind direction are 1138.44 m. The mean wind speed used to computed the delay in the wind speed between the wind turbines in the wind farm is

computed using a low pass filter with the transfer function:

$$H(s) = \frac{1}{s+1}.$$

The wake is modeled by a static wind deficit between the wind turbines by a factor of 0.9. This value is obtained by a modeling the wakes in this wind farm using the well know Jensen model, see [12], and then use the static values of the wake deficit. Turbulence of the wind is modeled in this model by random noise with a variance at 0.2, which is used to approximate realistic wind turbulence.

Since there is no dependency from the wind turbine/ wind farm control to the wind and wake model these two wind direction cases can be computed offline and are therefore provided in two .mat files: (winddata.mat winddata_case2.mat) at the web side mentioned above.

B. Wind Turbine Model

The wind turbine model used in this benchmark model is relatively simple. It represents each wind turbine as a closed loop system, where the model gives the responses on the three outputs (P_g , β , ω_g) to the two inputs (v_w and P_r). The parts in the model are developed to represent the closed loop wind turbine behavior. The model is based on a wind turbine model included in the wind farm model developed in [13].

This model consists of three parts: a power model, a pitch model and a generator speed model. They all consist of a number of approximating static functions and relations in frequency domain.

Power Model

The static available power $P_w(t)$ is given by (6). This power is the theoretical maximal generated power for the wind turbine.

$$P_w(t) = f_p(v_w(t)), \quad (6)$$

where $f_p(\cdot)$ is a static aerodynamic function.

Changes in the generated power will be instantaneous; therefore the static generated power is filtered by a first order transfer function to obtain the dynamically available power, $\hat{P}_w(t)$. This is defined in (7).

$$\hat{P}_w(s) = \frac{\tau_w(v_w)}{s + \alpha_w(v_w)} P_w(s), \quad (7)$$

where $\tau_w(v_w)$ is the transfer function coefficient which depends on the wind speed.

The wind turbine will as well work as a low pass filter to changes in the power reference to the wind turbine, $P_r(t)$. The actual dynamic response to the power reference, $\hat{P}_r(s)$ is computed by (8).

$$\hat{P}_r(s) = \frac{\tau_p}{s + \tau_p} P_r(s), \quad (8)$$

where τ_p is the transfer function coefficient.

The generated power, $P_c(t)$ is found by (9). As the available power of the wind turbine is lower than, the reference the wind turbine power is not limited by the power reference. However, in the case that the power reference is lower than the available power the generated power is subtracted by

the difference between the available power and the power reference.

$$P_c(t) = \hat{P}_w(t) - \text{pos}(\hat{P}_w(t) - \hat{P}_r(t)), \quad (9)$$

where $\text{pos}(\cdot)$ is a positive only function, which gives the input as output if the input is larger than 0, and 0 if not.

The generated electrical power, $P_g(t)$ is also influenced by oscillations in the wind turbine drive train this is modeled by a harmonic oscillation added to $P_c(t)$. $P_g(t)$ is given by (10).

$$P_g(t) = P_c(t) + \gamma_p \cdot \sin(\sigma_p \cdot 2 \cdot \pi \cdot t), \quad (10)$$

where γ_p is amplitude of the drive train oscillation and σ_p is the frequency of the drive train oscillation. Notice that the measured state of the generated electrical power is $P_g(t)$. Zero mean Gaussian random noise is added to $P_g(t)$ to represent measurement noises. Practical experiences have shown that a realistic value of the variance is $2.5 \cdot 10^5$ [W²].

Pitch Model: The actual dynamic pitch angle, $\beta(t)$ in the wind turbines is given in (11). It models the dynamic response of the pitch system in the wind turbine, by a first order transfer function of the pitch reference $\beta_r(t)$.

$$\beta(s) = \frac{\tau_\beta}{s + \tau_\beta} \beta_r(s), \quad (11)$$

where τ_β is the transfer function coefficient.

$\beta_r(t)$ is determined by a static aerodynamic function, $g(\cdot)$ which gives $\beta_r(t)$ depending on the ratio between $P_r(t)$ and the static theoretical available power, $P_a(t)$, and is given by (12).

$$P_a(t) = K_{pm} \cdot (v_w(t))^3. \quad (12)$$

If the available power is below the power reference for the wind turbine it should produce as much power as possible, but if the power reference is lower than the available power the generated power should be limited by increasing $\beta_r(t)$ to a follow the power reference to the wind turbine.

$$\beta_r(t) = g\left(\frac{P_r(t)}{h(v_w(t))}\right). \quad (13)$$

Measurement noise on the pitch position sensor is modeled as zero mean Gaussian random noise. Based on a proprietary sources the variance at 0.3 [o²] is used.

Generator Speed Model

The generator speed $\omega_g(t)$ increases as the $P_c(t)$ increases. Oscillations in the drive train will as well influence the generator speed. $\omega_g(t)$ is computed by a function $f_\omega(P_c(t))$ which gives $\omega_g(t)$ in the case of no oscillation. A harmonic function is introduced to represent the drive train oscillation, and the amplitude of the oscillation depends on the generator speed, therefore $f_\omega(P_c(t))$ is multiplied with the harmonic function added with 1. The expression of $\omega_g(t)$ is given by (14).

$$\omega_g(t) = f_\omega(P_c(t)) \left(1 + \frac{\gamma_\omega}{\omega_{g,\max}} \cdot \sin(\sigma_p \cdot 2 \cdot \pi \cdot t)\right), \quad (14)$$

where $\omega_{g,\max}$ is the maximal generator speed, and γ_ω is oscillation amplitude coefficient. Measurement noises on the

generator speed sensor is modeled by zero mean Gaussian noise by adding it to $\omega_g(t)$, with a variance at 0.1 [rad/s]^2 . The specific values of this measurement noise model are based on practical experiences.

C. Wind Farm Controller

The wind farm is modeled in continuous time since it is model of a physical system. The wind farm controller is, implemented in discrete time, as it is implemented on a computer, with a sample frequency at 0.1Hz. The power reference, $P_r[n]$, to one wind turbine is computed as given in (15).

$$P_r[n] = \frac{1}{9} \cdot \tilde{P}_{\text{wf,r}}[n], \quad (15)$$

where $\tilde{P}_{\text{wf,r}}[n]$ is the wind farm controllers power reference summarized of all wind turbines in the wind farm see (16). This controller introduces as well a low pass filter on the references changes to ensure slow variations on the power references.

$$\tilde{P}_{\text{wf,r}}(z) = \left(\frac{K_{\text{wf},1} T_s}{z-1} + K_{\text{wf},2} \right) \cdot (\tilde{P}_{\text{wf,r}}(z) - \tilde{P}_{\text{wf,g}}(z)), \quad (16)$$

where $\tilde{P}_{\text{wf,r}}(Z)$ is the power requested by the wind farm by the operator and $\tilde{P}_{\text{wf,g}}(Z)$ is the power generated by the wind farm. $\tilde{P}_{\text{wf,r}}[n]$ is limited to be within the interval 0 - 43.6 MW. (43.6 MW is given by the nine wind turbines in the wind farm with 4.8 MW as their nominal power).

The vector of power references, $\mathbf{P}_r[n]$ is given by (17).

$$\mathbf{P}_r[n] = \begin{bmatrix} P_{r11}[n] \\ P_{r12}[n] \\ P_{r13}[n] \\ P_{r21}[n] \\ P_{r22}[n] \\ P_{r23}[n] \\ P_{r31}[n] \\ P_{r32}[n] \\ P_{r33}[n] \end{bmatrix}. \quad (17)$$

Here, $P_{r11}[n]$ is the power reference to the wind turbine #1,1, and similar for the other elements in the vector of power references.

D. Model parameters

In this subsection the model parameters are provided. The parameters used in the fault models are selected such that they are realistic and as well challenging for detection and isolation. The parameters in the wind turbine model are found to matches the behavior of the wind turbine model used in [3].

Damage model for fault 2 $v_{\text{nom}} = 12.5 \text{ [m/s]}$, $K_{\gamma_2} = 1000 \text{ []}$

Damage model for fault 3 $K_{\gamma_3} = 100 \text{ []}$

Power model

f_p is a given as a look-up table, see Table I. $\tau_w(v_w)$ is given as a look-up table, see Table II. $\tau_p = 1.2 \text{ [rad/s]}$, $\gamma_p = 1000 \text{ [W]}$, $\sigma_p = 10 \text{ [Hz]}$.

Pitch model $\tau_\beta = 1.6 \text{ [rad/s]}$, $K_{\text{pm}} = 6.36 \cdot 10^3 \text{ [J/m}^3 \cdot \text{s}^2]$, and $g(\cdot)$ is given as a lookup table, see Table III.

Input	4.0	4.5	5.0	5.5	6.0
Output	0.0211	0.0461	0.0869	0.1469	0.2309
Input	6.5	7.0	7.5	8.0	8.5
Output	0.3422	0.4829	0.6600	0.8798	1.1323
Input	9.0	9.5	10.0		11.0
Output	1.4400	1.7770	2.1898	2.6501	3.1699
Input	11.5	12.0	12.5		
Output	3.7699	4.4002	4.8000		

TABLE I

LOOK UP TABLE FOR f_p . UNIT FOR INPUT [M/S] AND FOR OUTPUT [MW].

Input	4.0	4.5	5.0	5.5	6.0
Output	0.0274	0.0345	0.0405	0.0460	0.0512
Input	6.5	7.0	7.5	8.0	8.5
Output	0.0575	0.064	0.0697	0.077	0.0825
Input	9.0	9.5	10.0	10.5	11.0
Output	0.092	0.1	0.105	0.105	0.11
Input	11.5	12.0	12.5		
Output	0.115	0.115	0.115		

TABLE II

LOOK UP TABLE FOR $\tau_w(v_w)$. UNIT FOR INPUT [M/S] AND FOR OUTPUT [].

Generator speed model $\omega_{g,\text{max}} = 158 \text{ [rad/s]}$, $\gamma_\omega = 0.4 \text{ []}$, and f_ω is given as a lookup table, see Table IV.

Controller $K_{\text{wf},1} = 1 \text{ []}$, $K_{\text{wf},2} = 16 \text{ []}$, $T_s = 0.1 \text{ [s]}$.

V. TEST DEFINITION

Two different wind scenarios are included in the benchmark model, which corresponds to two different wind directions in the wind farm, 0° and 45° . These wind scenarios are pre-computed and is saved in winddata.mat and winddata_case2.mat respectively. In both cases Fault 1, 2 and 3 are occurring twice in three different wind turbines at different time intervals, i.e. no multiple faults are present. All faults occur once before and once after 2300 s. In the first period the wind farm cannot deliver the required power, which it can in the latter period.

Input	0.00075	0.0429	0.0483	0.0815	0.0943	0.11
Output	90	90	22	18	17	16.3
Input	0.129	0.153	0.1839	0.223	0.274	0.3453
Output	15.3	14.1	12.9	11.7	10.5	9.3
Input	0.44	0.4961	0.5669	0.5989	0.6335	0.6518
Output	7.5	6.7	6	5.6	5.2	4
Input	0.6707	0.6905	0.7945	1		
Output	4.7	4.5	0	0		

TABLE III

LOOK UP TABLE FOR $g(\cdot)$. UNIT FOR INPUT [] AND OUTPUT [$^\circ$].

Input	0.137	0.217	0.324	0.464	0.632	0.845
Output	48.3	56.2	64.3	72.4	80.5	88.5
Input	1.096	1.39	1.74	2.15	2.61	3.13
Output	96.6	104.7	112.8	120.8	128.9	137
Input	3.71	4.37	4.51	4.65	4.8	
Output	145.1	153.1	154.7	156.4	158	

TABLE IV

LOOK UP TABLE FOR $f_\omega(\cdot)$. UNIT FOR INPUT [MW] AND FOR OUTPUT [RAD/S]

Even though the wind sequences are fixed from simulation to simulation assuming the same wind scenario, the simulations still include a stochastic part by the zero mean Gaussian noise added to the three wind turbine outputs representing process noise and measurement noises in these closed loop systems. The general wind farm layout drawing, see Fig. 1,

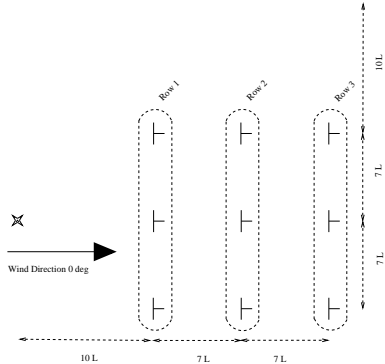


Fig. 4. Illustration of the example wind farm, in the case of 0 deg wind direction. The rows 1-3 are defined.

is now adjusted for the two scenarios illustrating the relevant description of the farm. A row in the wind farm is as well defined as a number of wind turbines on a straight line, where this line is orthogonal on the wind direction. The rows in the wind farm in case of 0 deg wind direction can be seen from Fig. 4, in which the three rows are defined. In case of the 45 deg wind direction, the 5 rows are defined by Fig. 5. The

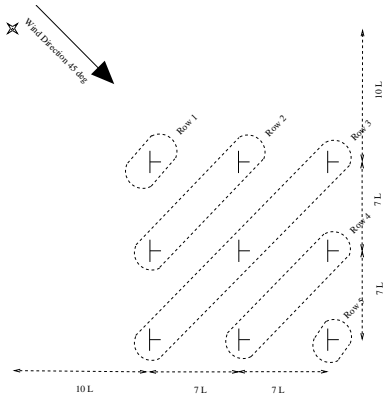


Fig. 5. Illustration of the example wind farm, in the case of 45 deg wind direction. The rows 1-5 are defined.

power reference to the wind farm $P_{wf,r}(t)$ is constant equal 43.6 MW until time equal 2000 s where it is lowered to be just above 30 MW in the rest of the time sequence.

A. Fault Cases

The three faults are active at different wind turbines at different times. Below it is described when and where the faults are present, and as well mentioned how they are modeled. All fault parameters are chosen based on experience, so that they are realistic and as well difficult to detect.

Fault 1: Fault 1, the debris build-up on the blades, is present from 1000 s to 1100 s in wind turbine number 3,1 and from 3000 s to 3100 s in wind turbine number 1,2. The

fault is modeled by scaling $P(t)$ obtained by (10). A scaling factor at 0.97 is used.

Fault 2: Fault 2, the pitch misalignment, is present from 1300 s to 1400 s in wind turbine number 1,1 and from 3300 s to 3400 s in wind turbine number 2,2. The fault is modeled by adding an offset at 0.3 deg to (11).

Fault 3: Fault 3, the decrease in drive train damping, is present 1600 s to 1700 s in wind turbine number 2,3 and from 3600 s to 3700 s in wind turbine number 3,2. This fault is modeled in two parts. It influences P and ω_g where it increases the oscillations in these variables. The change in P is introduced by increasing the amplitude of the sine function in (10) by a factor of 1.26. The change in ω_g is modeled by increasing the amplitude of the sine function in (14) by a factor of 2.3.

VI. SUMMARY

This paper presents a benchmark model for FDI as well as FTC of wind turbines in a wind farm on a wind farm level. The benchmark contains a simple model of a wind farm with nine wind turbines in which three relevant faults are introduced at three different time periods at different wind turbines. These faults are difficult to detect and isolate at the wind turbine level. However, it is expected that FDI and FTC algorithms at the wind farm control level would contribute to the detection, isolation and accommodation of these in a positive way.

REFERENCES

- [1] X. Wei, M. Verhaegen, and T. van den Engelen, "Sensor fault diagnosis of wind turbines for fault tolerant," in *Proceedings of the 17th World Congress The International Federation of Automatic Control*. Seoul, South Korea: IFAC, July 2008, pp. 3222–3227.
- [2] C. Sloth, T. Esbensen, and J. Stoustrup, "Active and passive fault-tolerant lpv control of wind turbines," in *Proceedings of the 2010 American Control Conference*, Baltimore, USA, June 2010, pp. 4640–4646.
- [3] P. Odgaard, J. Stoustrup, and M. Kinnaert, "Fault tolerant control of wind turbines a benchmark model," in *Proceedings of the 7th IFAC Symposium on Fault Detection, Supervision and Safety of Technical Processes*. Barcelona, Spain: IFAC, June–July 2009, pp. 155–160.
- [4] N. Laouti, N. Sheibat-Othman, and S. Othman, "Support vector machines for fault detection in wind turbines," in *Proceedings of IFAC World Congress 2011*, Milan, Italy, August–September 2011, pp. 7067–7072.
- [5] D. Rotondo, F. Nejjari, V. Puig, and J. Blesa, "Fault tolerant control of the wind turbine benchmark using virtual sensors/actuators," in *Proceedings of IFAC Safeprocess 2012*. Mexico City, Mexico: IFAC, August 2012, pp. 114–119.
- [6] A. Kusiak and A. Verma, "A data-driven approach for monitoring blade pitch faults in wind turbines," *IEEE Transactions on Sustainable Energy*, vol. 2, no. 1, pp. 87–96, January 2011.
- [7] P. Odgaard, "Competition on fault detection and fault tolerant control for wind farms," <http://www.kk-electronic.com/wind-turbine-control/competition-on-fault-detection/call-for-participation-part-iii.aspx>, 2012.
- [8] K. Johnson, M. Pao, L.Y. and Balas, and L. Fingersh, "Control of variable-speed wind turbines - standard and adaptive techniques for maximizing energy capture," *IEEE Control Systems Magazine*, vol. 26, no. 3, pp. 71–81, June 2006.
- [9] P. Odgaard and J. Stoustrup, "Results of a wind turbine fdi competition," in *Proceedings of Safeprocess 2012*. Mexico City, Mexico: IFAC, August 2012, pp. 102–107.
- [10] P. Odgaard, "Fault tolerant control of wind farm benchmark model," <http://www.kk-electronic.com/wind-turbine-control/competition-on-fault-detection/wind-farm-benchmark-model.aspx>, 2012.
- [11] T. Knudsen, T. Bak, and M. Soltani, "Prediction models for wind speed at turbine locations in a wind farm," *Wind Energy*, vol. 14, no. 7, pp. 877–894, October 2011.
- [12] N. Jensen, "A note on wind generation interaction," Risoe, Roskilde, Denmark, Tech. Rep. Risoe - M-2411, November 1983.
- [13] P. Odgaard, M. Baekgaard, and B. Astrup, "Model based control of wind parks," in *Proceedings of EWEA 2010*. Warsaw, Poland: EWEA, April 2010.